https://doi.org/10.48047/AFJBS.6.Si4.2024.356-377

African Journal of Biological Sciences

Analysis of some Topological indices at distance 2 of Carbon Nanotube $VC_5C_7[h,c]$

Kunjaru Mitra[1], Sunita Priya D'Silva[2], S.B. Chandrakala[3*], And B. Sooryanarayana[4]

[1*]Mangalore Institute of Technology and Engineering, Mangaluru, India, Email: mitrakunjaru@gmail.com
[2]Sahyadri College of Engineering and Management, Mangaluru, India, Email: sunitapriya11@gmail.com
[3]Nitte Meenakshi Institute of Technology, Bengaluru, India, Email: chandrakalasb14@gmail.com
[4]Dr. Ambedkar Institute of Technology,Bengaluru, India, Email: drsbsnrao.mat@drait.edu.in

***Corresponding Author**- *S. B.Chandrakala*
*Email: chandrakalasb14@gmail.com

Article History
Volume 6, Issue Si4, 2024
Received: 15 May 2024
Accepted: 05 June 2024
Published:1 July 2024
doi:
10.48047/AFJBS.6.Si4.2024.356-377

Abstract
Exploring into the area of advanced topological measures, the study significantly contributes to the exploration of complex networks, potentially enhancing ability to characterize their complexities with greater distinction and depth. In a manner akin to the topological indices developed by Gutman and Trinajstic, which rely on the vertex degrees within a network, broaden by introducing generalized topological indices by considering the degrees of vertices not just at immediate proximity but also at a distance of two edges. These indices offer a richer perspective on the network's structural dynamics, uncovering connectivity patterns that extend beyond direct neighbors. Also, a visual comparison of some topological indices for the $VC_5C_7(h,c)$ nanosheet is provided.

1 Introduction

Understanding carbon nanotubes involves paying attention to pivotal factors that significantly influence their physical and chemical properties. Among these factors, the shape and arrangement of atoms play a vital role. For example, the geometric shape of carbon nanotubes has a direct impact on their electrical structure. To delve into these properties, researchers use topological indices, which essentially provide a numerical description of how carbon atoms are organized in the nanotube structure. This information is particularly useful in predicting electronic features such as band structure, electronic density, and conductive behavior in carbon nanotubes.

Furthermore, topological indices are instrumental in assessing the chemical reactivity of carbon nanotubes. By understanding the arrangement of atoms and certain topological characteristics, researchers gain insights into the locations of chemical reactivity sites within the nanotube structure.

This knowledge is significant for various applications, including the development of nanotube-based materials and functionalization processes. Researchers use topological indices as quantitative descriptors to compare and categorize different carbon nanotube architectures based on their connections. This systematic examination helps in understanding the diversity among nanotube families. Moreover, the application of topological indices aids in the efficient screening of potential nanotube candidates for specific uses, such as electronics, sensors, and drug delivery. This approach provides a quicker alternative to intensive computer simulations, allowing researchers to anticipate certain properties of carbon nanotubes.

Beyond electronic properties, topological indices may also offer insights into other characteristics like mechanical strength, thermal conductivity, and optical qualities in carbon nanotubes. This comprehensive understanding of the relationships between topological indices and various properties is essential for designing nanotube-based materials with specific and desired characteristics.

Carbon has a special atomic structure that allows its electrons to participate in compounding, evolving such as $sp, sp^2$and sp^3. The diverse types of chemical bonds with distinct properties occur because of bonding of carbon within the molecules. The really interesting carbon material that comes from the unique structure of carbon atoms is called carbon sheets. These nanosheets are collection of carbon atoms complexly arranged in unique way at the tiny scale. These nanosheets are very flexible and stable, making them perfect for many uses and important for research endeavours. The essential strength, flexibility, and stability of carbon nanosheets contribute to their creativity and validity for various practical applications. Their unique nanoscale structures make them a favourable material for research in diverse fields. For a more in-depth examination of related work, additional information can be found in [17], [19]. Building on this generalization, we extend the concept by considering $l = 2$ for other existing topological indices. Specifically, we focus on the carbon nanosheet structure, denoted as $VC_5C_7[h, c]$, and computce various newly defined indices for this structure providing a detailed analysis. In 1972, Gutman and Trinajstic introduced Zagreb indices for molecular graphs. Later, researchers extended this concept, and in 2020, Sooryanarayana B, Chandrakala S.B, and Roshini G.R introduced a generalization of Zagreb indices at different distances. We further expand on this idea by applying it to existing topological indices, particularly focusing on the carbon nanosheet structure $VC_5C_7[h, c]$,and computing new indices for analysis.

2. Indices based on distance l.

In this section we extend generalization of [16] to some of the well known indices over the distance l between the two vertices of molecular graph rather than taking over edges of the molecular graph and are listed in Table 1.

Table 1: Definitions of topological indices at distance l

Sl.No.	Name of the indices	Notation and Definition
1	First Zagreb Index at distance l	${}_lM_1(G) = \sum_{d(u,v)=2} [\delta_G(u) + \delta_G(v)]$
2	Second Zagreb Index at distance l	${}_lM_2(G) = \sum_{d(u,v)=2} [\delta_G(u)\delta_G(v)]$
3	Harmonic Index at distance l	${}_lHI(G) = \sum_{d(u,v)=2} \frac{2}{\delta_G(u) + \delta_G(v)}$
4	Randic Index at distance l	${}_lR(G) = \sum_{d(u,v)=2} \frac{1}{\sqrt{\delta_G(u)\delta_G(v)}}$

5	Reciprocal Randic Index at distance l	${}_lRR(G) = \sum_{d(u,v)=2} \sqrt{\delta_G(u)\delta_G(v)}$
6	Sum Connectivity Index at distance l	${}_lSCI(G) = \sum_{d(u,v)=2} \frac{1}{\sqrt{\delta_G(u)+\delta_G(v)}}$
7	Nirmala Index at distance l	${}_lN(G) = \sum_{d(u,v)=2} \sqrt{\delta_G(u)+\delta_G(v)}$
8	Sombor Index at distance l	${}_lSO(G) = \sum_{d(u,v)=2} \sqrt{\delta_G(u)^2+\delta_G(v)^2}$
9	Modified Sombor index at distance l	${}^m_lSO(G) = \sum_{d(u,v)=2} \frac{1}{\sqrt{\delta_G(u)^2+\delta_G(v)^2}}$
10	Geometric–Arithmetic Index at distance l	${}_lGA(G) = \sum_{d(u,v)=2} \frac{2\sqrt{\delta_G(u)\delta_G(v)}}{\delta_G(u)+\delta_G(v)}$
11	Arithmetic–Geometric Index at distance l	${}_lAG(G) = \sum_{d(u,v)=2} \frac{\delta_G(u)+\delta_G(v)}{\sqrt{\delta_G(u)\delta_G(v)}}$
12	Atom Bond Connectivity Index at distance l	${}_lABC(G) = \sum_{d(u,v)=2} \sqrt{\frac{\delta_G(u)+\delta_G(v)-2}{\delta_G(u)\delta_G(v)}}$
13	Augmented Zagreb Index at distance l	${}_lAZI(G) = \sum_{d(u,v)=2} \left(\frac{\delta_G(u)\delta_G(v)}{\delta_G(u)+\delta_G(v)-2}\right)^2$
14	Inverse Sum Indeg Index at distance l	${}_lISI(G) = \sum_{d(u,v)=2} \frac{\delta_G(u)\delta_G(v)}{\delta_G(u)+\delta_G(v)}$
15	Redefined First Zagreb Index at distance l	${}_lReZg_1(G) = \sum_{d(u,v)=2} \frac{\delta_G(u)+\delta_G(v)}{\delta_G(u)\delta_G(v)}$

3. The Topological indices of the nanosheet $VC_5C_7[h,c]$

The molecular graph of nanotube $VC_5C_7[h,c]$ in which cycles C_5 and C_7 are combined in trivalent decoration to form a nanotube, which can be either a cylinder or a torus. In $2D$ graph of $VC_5C_7[h,c]$ nanosheet, we represent the number pentagons in the first row by c; here the first four rows of nodes and edges are alternatively repeated and the number of this recurrence is denoted by h. Let $N_1(h,c)$ (or N_1) denote $VC_5C_7[h,c]$. It can be seen from Figure 1 that the nanosheet $VC_5C_7[h,c]$ has $16hc+2h+5c$ vertices and $24hc+4c$ edges.

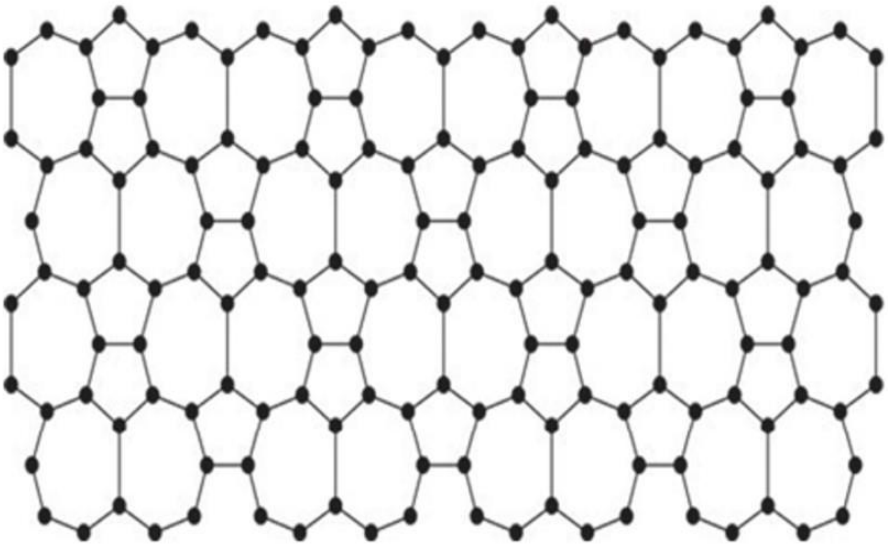

Figure 1: Nanosheet $VC_5C_7[2,4]$

The degree of vertices of molecular graph N_1 are of degree either 2 or 3. Let $P_{r,s}$ be the set of all uv–paths of length 2 in a graph such that $\delta(u) = r$ and $\delta(v) = s$. Thus N_1 contains $P_{2,2}$, $P_{2,3}$ and $P_{3,3}$. Number of elements of $P_{2,2}, P_{2,3}$ and $P_{3,3}$ of graph N_1 for $h, c \geq 2$ are listed in Tables 1, 2 and 3 respectively. Also the same is given for $N_1(1,c)$ and $N_1(h,1)$ where $h, c \geq 2$ are given in Table 5 and Table 6.

In this section we are computing different topological indices listed in Table 1 for the molecular graph of $VC_5C_7[h,c]$.

Table 2: $|P_{2,2}|$ of $VC_5C_7[h,c]$ where $h,c \geq 2$

Row/Column Number	1	2	…	c_{n-1}	c_n	Row Total
1	6	3		3	5	3c+5
2	2	–		–	2	4
…						
h_{n-1}	2	–		–	2	4
h_n	3	1		1	3	c+4
Column Total	$2h+5$	4	…	4	$2h+4$	$4h+4c+1$

Table 3: $|P_{2,3}|$ of $VC_5C_7[h,c]$ where $h,c \geq 2$

Row/Column Number	1	2	…	c_{n-1}	c_n	Row Total
1	10	6		6	10	6c+8

2	6	–		–	6	12
…						
h_{n-1}	6	–		–	6	12
h_n	12	10		10	12	10c+4
Column Total	$6h + 10$	16	…	16	$6h + 10$	$\boldsymbol{12h + 16c - 12}$

Table 4: $|P_{3,3}|$ of $VC_5C_7[h, c]$ where $h, c \geq 2$

Row/Column Number	1	2	…	c_{n-1}	c_n	**Row Total**
1	48	54		54	37	54c–23
2	42	48		48	32	48c–22
…						
h_{n-1}	42	48		48	32	48c–22
h_n	21	23		23	13	23c–12
Column Total	$42h - 15$	$48h - 19$	…	$48h - 19$	$32h - 14$	$\boldsymbol{48hc - 22h - 19c + 11}$

Table 5: Number of P_3's of $VC_5C_7[1, c]$, $c \geq 2$

$P_{r,s}$/ value of c	1	2	…	c_{n-1}	c_n	Total $\lvert P_{r,s}\rvert$
$\lvert P_{2,2}\rvert$	7	4		4	6	$4c + 5$
$\lvert P_{2,3}\rvert$	18	16		16	16	$16c + 2$
$\lvert P_{3,3}\rvert$	25	29		29	20	$29c - 13$

Table 6: Number of P_3's of $VC_5C_7[h,1]$, $h \geq 2$

Value of h/ $\lvert P_{r,s}\rvert$	$\lvert P_{2,2}\rvert$	$\lvert P_{2,3}\rvert$	$\lvert P_{3,3}\rvert$
1	8	14	22
2	4	8	26
...			
h_{n-1}	4	8	26
h_n	5	16	20
Total in each column	$4h+5$	$8h+14$	$\mathbf{26h-10}$

Now we summarise all the above tables to get total number of $\lvert P_{r,s}\rvert$ for every $r,s \in \{2,3\}$ in Table 7.

Table 7: Number of P_3's of $VC_5C_7[h,c]$, $h,c \geq 1$

Value of h, c $\lvert P_{r,s}\rvert$	$\lvert P_{2,2}\rvert$	$\lvert P_{2,3}\rvert$	$\lvert P_{3,3}\rvert$
$h=1, c\geq 2$	$4c+5$	$16c+2$	$29c-13$
$h\geq 2, c=1$	$4h+5$	$8h+14$	$26h-10$
$h,c\geq 2$	$4h+4c+1$	$12h+16c-12$	$48hc-22h-19c+11$

Theorem 3.1 *Let N_1 be a molecular graph of nanosheet $VC_5C_7[h,c]$ where $h,c \in Z^+$. Then*

$$(i)\quad {}_2M_1(N_1) = \begin{cases} 270c-48 & when\ h=1\ and\ c\geq 2 \\ 212h+30 & when\ c=1\ and\ h\geq 2 \\ 288hc-56h-18c+10 & when\ h\geq 2, c\geq 2 \end{cases}$$

$$(\text{ii})\ {}_2M_2(N_1) = \begin{cases} 373c-85 & when\ h=1\ and\ c\geq 2 \\ 298h+14 & when\ c=1\ and\ h\geq 2 \\ 432hc-110h-59c+31 & when\ h\geq 2, c\geq 2 \end{cases}$$

$$(\text{iii})\ {}_2HI(N_1) = \begin{cases} \frac{271}{15}c-\frac{31}{30} & when\ h=1\ and\ c\geq 2 \\ \frac{208}{15}h+\frac{143}{30} & when\ c=1\ and\ h\geq 2 \\ 16hc+\frac{22}{15}h+\frac{61}{15}-\frac{2}{15} & when\ h\geq 2, c\geq 2 \end{cases}$$

Proof. (i) From Table 1, we have ${}_2M_1(N_1) = \sum_{d(u,v)=2}[\delta_G(u)+\delta_G(v)] = |P_{2,2}|(4)+|P_{2,3}|(5)+|P_{3,3}|(6)$. Further proof is discussed based on the values of h and c using Table 7.

a)when $h = 1$ and $c \geq 2$
we get, ${}_2M_1(N_1) = (4c + 5)(4) + (16c + 2)(5) + (29c - 13)(6) = 270c - 48.$

b) when $c = 1$ and $h \geq 2$
we get, ${}_2M_1(N_1) = (4h + 5)(4) + (8h + 14)(5) + (26h - 10)(6) = 212h + 30.$

c) when both $h, c \geq 2$
we get, ${}_2M_1(N_1) = 4(4h + 4c + 1) + 5(12h + 16c - 12) + 6(48hc - 22h - 19c + 11)$
${}_2M_1(N) = 288hc - 56h - 18c + 10.$

(ii) From Table 1, we have ${}_2M_2(N_1) = \sum_{d(u,v)=2} [\delta_G(u)\delta_G(v)] = |P_{2,2}|(4) + |P_{2,3}|(6) + |P_{3,3}|(9)$. Further proof is discussed based on the values of h and c using Table 7.

a)when $h = 1$ and $c \geq 2$
we get ${}_2M_2(N_1) = (4c + 5)(4) + (16c + 2)(6) + (29c - 13)(9) = 373c - 85.$

b) when $c = 1$ and $h \geq 2$
we get, ${}_2M_2(N_1) = (4h + 5)(4) + (8h + 14)(6) + (26h - 10)(9) = 298h + 14.$

c) when $h \geq 2, c \geq 2$
we get, ${}_2M_2(N_1) = (4h + 4c + 1)(4) + (12h + 16c - 12)(6) + (48hc - 22h - 19c + 11)(9)$
${}_2M_2(N) = 432hc - 110h - 59c + 31.$

(iii) From Table 1, we have ${}_2HI(N_1) = \sum_{d(u,v)=2} \frac{2}{\delta_G(u)+\delta_G(v)} = \frac{2}{4}|P_{2,2}| + \frac{2}{5}|P_{2,3}| + \frac{2}{6}|P_{3,3}|$. Further proof is discussed based on the values of h and c using Table 7.

a)when $h = 1$ and $c \geq 2$
we get, ${}_2HI(N_1) = 2(\frac{1}{4}(4c + 5) + \frac{1}{5}(16c + 2) + \frac{1}{6}(29c - 13)) = \frac{271}{15}c - \frac{31}{30}.$

b) when $c = 1$ and $h \geq 2$
we get, ${}_2HI(N_1) = 2(\frac{1}{4}(4h + 5) + \frac{1}{5}(8h + 14) + \frac{1}{6}(26h - 10)) = \frac{208}{15}h + \frac{143}{30}.$

c) when $h \geq 2, c \geq 2$
we get, ${}_2HI(N_1) = 2(\frac{2}{4}(4h + 4c + 1) + \frac{1}{5}(12h + 16c - 12) + \frac{1}{6}(48hc - 22h - 19c + 11))$
${}_2HI(N_1) = 16hc + \frac{22}{15}h + \frac{61}{15} - \frac{2}{15}.$

Theorem 3.2 *Let N_1 be a molecular graph of Nanotube $VC_5C_7[h, c]$ where $h, c \in Z^+$. Then*

$$(i) \quad {}_2R(N_1) = \begin{cases} 18.1986c - 1.0168 & when\ h = 1\ and\ c \geq 2 \\ 3.4968h + 4.8821 & when\ c = 1\ and\ h \geq 2 \\ 16hc - 0.4344h - 2.1986c - 0.7323 & when\ h \geq 2, c \geq 2 \end{cases}$$

$$(ii) \quad {}_2RR(N_1) = \begin{cases} 134.1918c - 24.1010 & when\ h = 1\ and\ c \geq 2 \\ 105.5959h + 14.2929 & when\ c = 1\ and\ h \geq 2 \\ 144hc - 28.6061h - 9.8081c + 5.6061 & when\ h \geq 2, c \geq 2 \end{cases}$$

Proof.(i) From Table 1, we have ${}_2R(N_1) = \sum_{d(u,v)=2} \frac{1}{\sqrt{\delta_G(u)\delta_G(v)}} = \frac{1}{\sqrt{4}}|P_{2,2}| + \frac{1}{\sqrt{6}}|P_{2,3}| + \frac{1}{\sqrt{9}}|P_{3,3}|$. Further proof is discussed based on the values of h and c using Table 7.

a)when $h = 1$ and $c \geq 2$

$$ {}_2R(N_1) = \frac{1}{2}(4c+5) + \frac{1}{\sqrt{6}}(16c+2) + \frac{1}{3}(29c-13)$$

$$ {}_2R(N_1) = (\tfrac{35+8\sqrt{6}}{3})c + (\tfrac{-11+2\sqrt{6}}{6}) = 18.1986c - 1.0168.$$

b) when $c = 1$ and $h \geq 2$

$$ {}_2R(N_1) = \frac{1}{2}(4h+5) + \frac{1}{\sqrt{6}}(8h+14) + \frac{1}{3}(26h-10)$$

$$ {}_2R(N_1) = \left(\tfrac{32+4\sqrt{6}}{3}\right) + \left(\tfrac{-5+14\sqrt{6}}{6}\right) = 13.9327h + 4.8821$$

c) when $h, c \geq 2$

$$ {}_2R(N_1) = \frac{1}{2}(4h+4c+1) + \frac{1}{\sqrt{6}}(12h+16c-12) + \frac{1}{3}(48hc-22h-19c+11)$$

$$= 16hc + (\tfrac{-16+6\sqrt{6}}{3})h + (\tfrac{-13+8\sqrt{6}}{3})c + (\tfrac{25-12\sqrt{6}}{6}) = 16hc - 0.4344h - 2.1986c - 0.7323.$$

(ii) From Table 1, we have ${}_2RR(N) = \sum_{d(u,v)=2} \sqrt{\delta_G(u)\delta_G(v)} = \sqrt{4}|P_{2,2}| + \sqrt{6}|P_{2,3}| + \sqrt{9}|P_{3,3}|$. Further proof is discussed based on the values of h and $c$using Table 7.

a)when $h = 1$ and $c \geq 2$

$$ {}_2RR(N_1) = 2(4c+5) + \sqrt{6}(16c+2) + 3(29c-13) = (95+16\sqrt{6})c + (-29+2\sqrt{6})$$

$$ {}_2RR(N_1) = 134.1918c - 24.1010.$$

b) when $c = 1$ and $h \geq 2$

$$ {}_2RR(N_1) = 2(4h+5) + \sqrt{6}(8h+14) + 3(26h-10) = (86+8\sqrt{6})h + (-20+14\sqrt{6})$$

$$ {}_2RR(N_1) = 105.5959h + 14.2929.$$

c) when $h, c \geq 2$

$$ {}_2RR(N_1) = 2(4h+4c+1) + \sqrt{6}(12h+16c-12) + 3(48hc-22h-19c+11)$$

$$= 144hc + (-58+12\sqrt{6})h + (-49+16\sqrt{6})c + 35 - 12\sqrt{6} = 144hc - 28.6061h - 9.8081c + 5.6061.$$

Theorem 3.3 *Let N_1 be a molecular graph of Nanotube $VC_5C_7[h,c]$ where $h, c \in Z^+$. Then*

$$(i) \quad {}_2SCI(N_1) = \begin{cases} 20.9946c - 1.9128 & when\ h = 1\ and\ c \geq 2 \\ 16.1921h + 4.6785 & when\ c = 1\ and\ h \geq 2 \\ 8\sqrt{6}hc - 1.6149h + 1.3987c - 0.3758 & when\ h \geq 2, c \geq 2 \end{cases}$$

$$(ii) \quad {}_2N(N_1) \begin{cases} 128.4023c - 5.8992 & when\ h = 1\ and\ c \geq 2 \\ 89.5752h + 16.81 & when\ c = 1\ and\ h \geq 2 \\ 48\sqrt{6}hc - 19.0559h - 2.7632c + 2.1116 & when\ h \geq 2, c \geq 2 \end{cases}$$

Proof.(i) From Table 1, we have

$${}_2SCI(N_1) = \sum_{d(u,v)=2} \frac{1}{\sqrt{\delta_G(u)+\delta_G(v)}} = \frac{1}{\sqrt{4}}|P_{2,2}| + \frac{1}{\sqrt{5}}|P_{2,3}| + \frac{1}{\sqrt{6}}|P_{3,3}|.$$

Further proof is discussed based on the values of h and c using Table 7.

a) when $h = 1$ and $c \geq 2$

$$ {}_2SCI(N_1) = \frac{1}{2}(4c+5) + \frac{1}{\sqrt{5}}(16c+2) + \frac{1}{\sqrt{6}}(29c-13)$$

$$ {}_2SCI(N_1) = (2 + \tfrac{16}{\sqrt{5}} + \tfrac{29}{\sqrt{6}})c + (\tfrac{5}{2} + \tfrac{2}{\sqrt{5}} - \tfrac{13}{\sqrt{6}}) = 20.9946c - 1.9128. $$

b) when $c = 1$ and $h \geq 2$

$$ {}_2SCI(N_1) = \frac{1}{2}(4h + 5) + \frac{1}{\sqrt{5}}(8h + 14) + \frac{1}{\sqrt{6}}(26h - 10) $$

$$ {}_2SCI(N_1) = (2 + \tfrac{8}{\sqrt{5}} + \tfrac{26}{\sqrt{6}})h + (\tfrac{5}{2} + \tfrac{14}{\sqrt{5}} - \tfrac{10}{\sqrt{6}}) = 16.1921h + 4.6785. $$

c) when $h, c \geq 2$

$$ {}_2SCI(N_1) = \frac{1}{2}(4h + 4c + 1) + \frac{1}{\sqrt{5}}(12h + 16c - 12) + \frac{1}{\sqrt{6}}(48hc - 22h - 19c + 11) $$

$$ {}_2SCI(N_1) = 8\sqrt{6}hc + \left(2 + \frac{12}{\sqrt{5}} - \frac{22}{\sqrt{6}}\right)h + \left(2 + \frac{16}{\sqrt{5}} - \frac{19}{\sqrt{6}}\right)c + \left(0.5 - 12\sqrt{5} + \frac{11}{\sqrt{6}}\right) $$

$$ = 8\sqrt{6}hc - 1.6149h + 1.3987c - 0.3758. $$

(ii) From Table 1, we have ${}_2N(N_1) = \sum_{d(u,v)=2} \sqrt{\delta_G(u) + \delta_G(v)} = \sqrt{4}|P_{2,2}| + \sqrt{5}|P_{2,3}| + \sqrt{6}|P_{3,3}|$. Further proof is discussed based on the values of h and c using Table 7.

a)when $h = 1$ and $c \geq 2$

$$ {}_2N(N_1) = 2(4c + 5) + \sqrt{5}(16c + 2) + \sqrt{6}(29c - 13) $$

$$ {}_2N(N_1) = (8 + 16\sqrt{5} + 29\sqrt{6})c + (10 + 2\sqrt{5} - 13\sqrt{6}) = 114.8122c - 17.3712. $$

b) when $c = 1$ and $h \geq 2$

$$ {}_2N(N_1) = 2(4h + 5) + \sqrt{5}(8h + 14) + \sqrt{6}(26h - 10) $$

$$ {}_2N(N_1) = (8 + 8\sqrt{5} + 26\sqrt{6})h + (10 + 14\sqrt{5} - 10\sqrt{6}) = 89.5752h + 16.81. $$

c) when $h, c \geq 2$

$$ {}_2N(N_1) = 2(4h + 4c + 1) + \sqrt{5}(12h + 16c - 12) + \sqrt{6}(48hc - 22h - 19c + 11) $$

$$ {}_2N(N_1) = 48\sqrt{6}hc + (8 + 12\sqrt{5} - 22\sqrt{6})h + (8 + 16\sqrt{5} - 19\sqrt{6})c + (2 - 12\sqrt{5} + 11\sqrt{6}) $$

$$ {}_2N(N_1) = 48\sqrt{6}hc - 19.0559h - 2.7632c + 2.1116. $$

Theorem 3.4 *Let N_1 be a molecular graph of Nanotube $VC_5C_7[h, c]$ where $h, c \in Z^+$. Then*

$$ (i) \quad {}_2SO(N_1)\begin{cases} 192.0391c - 33.8011 & when\ h = 1\ and\ c \geq 2 \\ 150.4667h + 22.1934 & when\ c = 1\ and\ h \geq 2 \\ 203.6467hc - 38.7578h - 11.6076c + 6.2309 & when\ h \geq 2, c \geq 2 \end{cases} $$

$$ (ii) \quad {}^m_2SO(N_1) = \begin{cases} 12.6872c - 0.7417 & when\ h = 1\ and\ c \geq 2 \\ 9.7612h + 3.2936 & when\ c = 1\ and\ h \geq 2 \\ 8\sqrt{2}hc - 0.4430h + 1.3735c - 0.3319 & when\ h \geq 2, c \geq 2 \end{cases} $$

Proof. (i) From Table 1, we have ${}_2SO(N_1) = \sum_{d(u,v)=2} \sqrt{\delta_G(u)^2 + \delta_G(v)^2} = \sqrt{8}|P_{2,2}| + \sqrt{13}|P_{2,3}| + \sqrt{18}|P_{3,3}|$. Further proof is discussed based on the values of h and c using Table 7.

a)when $h = 1$ and $c \geq 2$

$$ {}_2SO(N_1) = 2\sqrt{2}(4c + 5) + \sqrt{13}(16c + 2) + 3\sqrt{2}(29c - 13) $$

$$ {}_2SO(N_1) = (95\sqrt{2} + 16\sqrt{13})c + (-29\sqrt{2} + 2\sqrt{13}) = 192.0391c - 33.8011. $$

b) when $c = 1$ and $h \geq 2$

$$ {}_2SO(N_1) = 2\sqrt{2}(4h + 5) + \sqrt{13}(8h + 14) + 3\sqrt{2}(26h - 10) $$

$$ {}_2SO(N_1) = (86\sqrt{2} + 8\sqrt{13})c + (-20\sqrt{2} + 14\sqrt{13}) = 150.4667h + 22.1934. $$

c) when $h, c \geq 2$

$$_2SO(N_1) = 2\sqrt{2}(4h + 4c + 1) + \sqrt{13}(12h + 16c - 12) + 3\sqrt{2}(48hc - 22h - 19c + 11)$$
$$_2SO(N_1) = 144\sqrt{2}hc + (-58\sqrt{2} + 12\sqrt{13})h + (-49\sqrt{2} + 16\sqrt{13})c + 35\sqrt{2} - 12\sqrt{13}$$
$$_2SO(N_1) = 203.6467hc - 38.7578h - 11.6076c + 6.2309$$

(ii) From Table 1, we have

$$_2^mSO(N_1) = \sum_{d(u,v)=2} \frac{1}{\sqrt{\delta_G(u)^2+\delta_G(v)^2}} = \frac{1}{\sqrt{8}}|P_{2,2}| + \frac{1}{\sqrt{13}}|P_{2,3}| + \frac{1}{\sqrt{18}}|P_{3,3}|.$$

Further proof is discussed based on the values of h and $c$using Table 7.

a)when $h = 1$ and $c \geq 2$

$$_2^mSO(N_1) = \frac{1}{2\sqrt{2}}(4c + 5) + \frac{1}{\sqrt{13}}(16c + 2) + \frac{1}{3\sqrt{2}}(29c - 13)$$
$$_2^mSO(N_1) = (\frac{35}{3\sqrt{2}} + \frac{16}{\sqrt{13}})c + (\frac{-11}{6\sqrt{2}} + \frac{2}{\sqrt{13}}) = 12.6872c - 0.7417.$$

b) when $c = 1$ and $h \geq 2$

$$_2^mSO(N_1) = \frac{1}{2\sqrt{2}}(4h + 5) + \frac{1}{\sqrt{13}}(8h + 14) + \frac{1}{3\sqrt{2}}(26h - 10)$$
$$_2^mSO(N_1) = (\frac{32}{3\sqrt{2}} + \frac{8}{\sqrt{13}})h + (\frac{-5}{6\sqrt{2}} + \frac{14}{\sqrt{13}}) = 9.7612h + 3.2936.$$

c) when $h, c \geq 2$

$$_2^mSO(N_1) = \frac{1}{2\sqrt{2}}(4h + 4c + 1) + \frac{1}{\sqrt{13}}(12h + 16c - 12) + \frac{1}{3\sqrt{2}}(48hc - 22h - 19c + 11)$$
$$_2^mSO(N_1) = 8\sqrt{2} + (\frac{-16}{3\sqrt{2}} + \frac{12}{\sqrt{13}})h - (\frac{-13}{3\sqrt{2}} + \frac{16}{\sqrt{13}})c + (\frac{25}{6\sqrt{2}} + \frac{-12}{\sqrt{13}})$$
$$_2^mSO(N_1) = 8\sqrt{2}hc - 0.4430h + 1.3735c - 0.3319.$$

Theorem 3.5 *Let N_1 be a molecular graph of Nanotube $VC_5C_7[h, c]$ where $h, c \in Z^+$. Then*

$$(i) \quad _2GA(N_1)\begin{cases} 48.6767c - 6.0404 & when\ h = 1\ and\ c \geq 2 \\ 37.8384h + 8.7171 & when\ c = 1\ and\ h \geq 2 \\ 48hc - 6.2424h + 0.6767c + 0.2425 & when\ h \geq 2, c \geq 2 \end{cases}$$

$$(ii) \quad _2ABC(N_1)\begin{cases} 33.4754c - 3.7169 & when\ h = 1\ and\ c \geq 2 \\ 25.8186h + 6.7683 & when\ c = 1\ and\ h \geq 2 \\ 32hc - 3.3529h + 1.4754c - 0.4448 & when\ h \geq 2, c \geq 2 \end{cases}$$

$$(iii) \quad _2AG(N_1)\begin{cases} 98.6598c - 11.9175 & when\ h = 1\ and\ c \geq 2 \\ 76.3299h + 18.5773 & when\ c = 1\ and\ h \geq 2 \\ 96hc - 11.5051h + 2.6598c - 0.4949 & when\ h \geq 2, c \geq 2 \end{cases}$$

Proof.(i) From Table 1, we have

$$_2GA(N_1) = \sum_{d(u,v)=2} \frac{2\sqrt{\delta_G(u)\delta_G(v)}}{\delta_G(u)+\delta_G(v)} = \frac{2\sqrt{4}}{4}|P_{2,2}| + \frac{2\sqrt{6}}{5}|P_{2,3}| + \frac{2\sqrt{9}}{6}|P_{3,3}|.$$

Further proof is discussed based on the values of h and c using Table 7.

a)when $h = 1$ and $c \geq 2$

$$_2GA(N_1) = (4c + 5) + \frac{2\sqrt{6}}{5}(16c + 2) + (29c - 13) = (33 + \frac{32\sqrt{6}}{5})c + (-8 + \frac{4\sqrt{6}}{5}) = 48.6767c - 6.0404$$

b) when $c = 1$ and $h \geq 2$

$$_2GA(N_1) = (4h + 5) + \frac{2\sqrt{6}}{5}(8h + 14) + (26h - 10) = (30 + \frac{16\sqrt{6}}{5})h + (-5 + \frac{28\sqrt{6}}{5}) = 37.8384h +$$

8.7171.

c) when $h, c \geq 2$

$$ {}_2GA(N_1) = (4h + 4c + 1) + \frac{2\sqrt{6}}{5}(12h + 16c - 12) + (48hc - 22h - 19c + 11)$$
$$= 48hc + \left(-18 + \tfrac{24\sqrt{6}}{5}\right)h + \left(-15 + \tfrac{32\sqrt{6}}{5}\right)c + \left(12 - \tfrac{24\sqrt{6}}{5}\right) = 48hc - 6.2424h + 0.6767c + 0.2425.$$

(ii) ${}_2ABC(N_1) = \sum_{d(u,v)=2}\sqrt{\frac{\delta_G(u)+\delta_G(v)-2}{\delta_G(u)\delta_G(v)}} = \sqrt{\frac{2+2-2}{4}}|P_{2,2}| + \sqrt{\frac{2+3-2}{6}}|P_{2,3}| + \sqrt{\frac{3+3-2}{9}}|P_{3,3}|$. Further proof is discussed based on the values of h and c using Table 7.

a)when $h = 1$ and $c \geq 2$

$$ {}_2ABC(N_1) = \tfrac{1}{\sqrt{2}}(4c + 5) + \tfrac{1}{\sqrt{2}}(16c + 2) + \tfrac{2}{3}(29c - 13)$$
$$= \left(\frac{20}{\sqrt{2}} + \frac{58}{3}\right)c + \left(\frac{7}{\sqrt{2}} - \frac{26}{3}\right)$$
$$= 33.4754c - 3.7169$$

b) when $c = 1$ and $h \geq 2$

$$ {}_2ABC(N_1) = \tfrac{1}{\sqrt{2}}(4h + 5) + \tfrac{1}{\sqrt{2}}(8h + 14) + \tfrac{2}{3}(26h - 10)$$
$$= (\frac{12}{\sqrt{2}} + \frac{52}{3})h + (\frac{19}{\sqrt{2}} - \frac{20}{3}) = 25.8186h + 6.7683$$

c) when $h \geq 2, c \geq 2$

$$ {}_2ABC(N_1) = \tfrac{1}{\sqrt{2}}(4h + 4c + 1) + \tfrac{1}{\sqrt{2}}(12h + 16c - 12) + \tfrac{2}{3}(48hc - 22h - 19c + 11)$$
$$= 32hc + \left(\frac{16}{\sqrt{2}} - \frac{44}{3}\right)h + \left(\frac{20}{\sqrt{2}} - \frac{38}{3}\right)c + \left(\frac{-11}{\sqrt{2}} + \frac{22}{3}\right)$$
$$= 32hc - 3.3529h + 1.4754c - 0.4448$$

(iii) From Table 1, we have ${}_2AG(N_1) = \sum_{d(u,v)=2}\sum_{d(u,v)=2}\frac{\delta_G(u)+\delta_G(v)}{\sqrt{\delta_G(u)\delta_G(v)}} = \frac{4}{\sqrt{4}}|P_{2,2}| + \frac{5}{\sqrt{6}}|P_{2,3}| + \frac{6}{\sqrt{9}}|P_{3,3}|$. Further proof is discussed based on the values of h and $c$using Table 7.

a)when $h = 1$ and $c \geq 2$

$$ {}_2AG(N_1) = 2(4c + 5) + \frac{5}{\sqrt{6}}(16c + 2) + 2(29c - 13)$$
$$= \left(66 + \frac{80}{\sqrt{6}}\right)c - \left(16 - \frac{10}{\sqrt{6}}\right)$$
$$= 98.6598c - 11.9175.$$

b) when $c = 1$ and $h \geq 2$

$$ {}_2AG(N_1) = 2(4h + 5) + \frac{5}{\sqrt{6}}(8h + 14) + 2(26h - 10)$$
$$= \left(60 + \frac{40}{\sqrt{6}}\right)h + \left(-10 + \frac{70}{\sqrt{6}}\right)$$
$$= 76.3299h + 18.5773$$

c) when $h, c \geq 2$

$$ {}_2AG(N_1) = 2(4h + 4c + 1) + \frac{5}{\sqrt{6}}(12h + 16c - 12) + 2(48hc - 22h - 19c + 11)$$
$$= 96hc + \left(-36 + \frac{60}{\sqrt{6}}\right)h + \left(-30 + \frac{80}{\sqrt{6}}\right)c + \left(24 - \frac{60}{\sqrt{6}}\right)$$
$$= 96hc - 11.5051h + 2.6598c - 0.4949.$$

Theorem 3.6 *Let N_1 be a molecular graph of Nanotube $VC_5C_7[h, c]$ where $h, c \in Z^+$. Then*

$$(i)\quad {}_2AZI(N_1)\begin{cases}490.3281c-92.0781 & when\ h=1\ and\ c\geq 2\\ 392.15625h+38.0937 & when\ c=1\ and\ h\geq 2\\ 546.75hc-122.5938h-56.4219c+37.2969 & when\ h\ \geq\ 2, c\geq\ 2\end{cases}$$

$$(ii)\quad {}_2ISI(N_1)=\begin{cases}66.7c-12.1 & when\ h=1\ and\ c\geq 2\\ 52.6h+6.8 & when\ c=1\ and\ h\geq 2\\ 72hc-14.6h-5.3c+3.1 & when\ h\ \geq\ 2, c\geq\ 2\end{cases}$$

$$(iii){}_2ReZg(N_1)\begin{cases}36.6667c-2 & when\ h=1\ and\ c\geq 2\\ 28h+10 & when\ c=1\ and\ h\geq 2\\ 32hc-0.6667h+4.6667c-1.6667 & when\ h\ \geq\ 2, c\geq\ 2\end{cases}$$

Proof. (i) From Table 1, we have

${}_2AZI(N_1)=\sum_{d(u,v)=2}\left(\frac{\delta_G(u)\delta_G(v)}{\delta_G(u)+\delta_G(v)-2}\right)^3=\left(\frac{4}{2+2-2}\right)^3|P_{2,2}|+\left(\frac{6}{2+3-2}\right)^3|P_{2,3}|+\left(\frac{9}{3+3-2}\right)^3|P_{3,3}|.$

Further proof is discussed based on the values of h and c using Table 7.

a)when $h=1$ and $c\geq 2$

$$ {}_2AZI(N_1)=8(4c+5)+8(16c+2)+\left(\frac{9}{4}\right)^3(29c-13)$$
$$=\frac{1}{64}(31381c-5893)=490.3281c-92.$$

b) when $c=1$ and $h\geq 2$

$$ {}_2AZI(N_1)=8(4h+5)+8(8h+14)+\left(\frac{9}{4}\right)^3(26h-10)$$
$$=\tfrac{1}{32}(12549h-1219)=392.15625h+38.0937.$$

c) when $h\geq 2, c\geq 2$

$$ {}_2AZI(N_1)=8(4h+4c+1)+8(12h+16c-12)+\left(\frac{9}{4}\right)^3(48hc-22h-19c+11)$$
$$=\frac{2187}{4}hc-\frac{3923}{32}h-\frac{3611}{64}c+\frac{2387}{64}=546.75hc-122.5938h-56.4219c+37.2969.$$

(ii) From Table 1, we have ${}_2ISI(N_1)=\sum_{d(u,v)=2}\frac{\delta_G(u)\delta_G(v)}{\delta_G(u)+\delta_G(v)}=\frac{4}{4}|P_{2,2}|+\frac{6}{5}|P_{2,3}|+\frac{9}{6}|P_{3,3}|$

Further proof is discussed based on the values of h and c using Table 7.

a)when $h=1$ and $c\geq 2$

$$ {}_2ISI(N_1)=(4c+5)+\frac{6}{5}(16c+2)+\frac{3}{2}(29c-13)=\frac{667}{10}c-\frac{121}{10}=66.7c-12.1$$

b) when $c=1$ and $h\geq 2$

$$ {}_2ISI(N_1)=(4h+5)+\tfrac{6}{5}(8h+14)+\tfrac{3}{2}(26h-10)=\tfrac{263}{5}h+\tfrac{34}{5}=52.6h+6.8.$$

c) when $h\geq 2, c\geq 2$

$$ {}_2ISI(N_1)=(4h+4c+1)+\tfrac{6}{5}(12h+16c-12)+\tfrac{3}{2}(48hc-22h-19c+11)$$
$$=72hc-\frac{73}{5}h-\frac{53}{10}c+\frac{31}{10}=72hc-14.6h-5.3c+3.1.$$

(iii) From Table 1, we have ${}_2ReZg_1(N_1)=\sum_{d(u,v)=2}\frac{\delta_G(u)+\delta_G(v)}{\delta_G(u)\delta_G(v)}=\frac{4}{4}|P_{2,2}|+\frac{5}{6}|P_{2,3}|+\frac{2}{3}|P_{3,3}|.$

Further proof is discussed based on the values of h and c using Table 7.

a)when $h=1$ and $c\geq 2$

$$ {}_2ReZg_1(N_1)=(4c+5)+\frac{5}{6}(16c+2)+\frac{2}{3}(29c-13)=\frac{110}{3}c-2=36.6667c-2.$$

b) when $c = 1$ and $h \geq 2$

$$_2ReZg_1(N_1) = (4h + 5) + \frac{5}{6}(8h + 14) + \frac{2}{3}(26h - 10) = 28h + 10$$

c) when $h \geq 2, c \geq 2$

$$_2ReZg_1(N_1) = (4h + 4c + 1) + \frac{5}{6}(12h + 16c - 12) + \frac{2}{3}(48hc - 22h - 19c + 11)$$
$$= 32hc - 0.6667h + \frac{14}{3}c - \frac{5}{3} = 32hc - 0.6667h + 4.6667c - 1.6667.$$

From the data given in the [4], we have computed the TI's of for distance one and are listed in Table 8. For more details we refer [4], [3],[7], [10], [12]. We compare it to the results of two distance topological indices established in this study.

Table 8: Topological indices of $VC_5C_7[h, c]$, $h, c \geq 2$ at distance 1

Sl.No.	Name of the indices	TI's for N_1
1	First Zagreb Index	$M_1(N_1) = 10c - 12h + 144hc.$
2	Second Zagreb Index	$M_2(N_1) = 216hc - 4c - 34h + 4.$
3	Harmonic Index	$HI(N_1) = 8hc + 0.8666h + 2.3333c + 0.1333$
4	Randic Index	$R(N_1) = 8hc - 0.2340h + 2.4158c + 0.0673$
5	Reciprocal Randic Index	$RR(N_1) = 72hc - 6.404h - 5.8579c + 0.4041$
6	Sum Connectivity Index	$SCI(N_1) = 4\sqrt{6}hc + 0.4952h + 0.2061c + 0.0553$
7	Nirmala Index	$N(N_1) = 24\sqrt{6}hc - 2.6063h + 6.7648c - 0.0906$
8	Sombor Index	$SO(N_1) = 72\sqrt{2}hc - 7.9251h + 7.7712c - 0.5601$
9	Modified Sombor index	$^mSO(N_1) = 4\sqrt{2}hc + 0.5689h + 1.5949c + 0.1382$
10	Geometric–Arithmetic Index	$GA(N_1) = 24hc - 2.9677h + 6.3129c + 0.2708$
11	Arithmetic–Geometric Index	$AG(N_1) = 48hc + 0.3299h + 8.4124c - 4.3299$
12	Atom Bond Connectivity Index	$ABC(N_1) = 16hc + 0.4044h + 3.1519c - 0.1676$
13	Augmented Zagreb Index	$AZI(N_1) = 273.375hc - 33.90623h + 4.875c + 13.5625$
14	Inverse Sum Indeg Index	$ISI(N_1) = 36hc - 3.4h + 2.5c - 0.6$
15	Redefined First Zagreb Index	$ReZg_1(N_1) = 16hc + 2h + 5c$

4 Graphs and Analysis of TI's of $N_1 = VC_5C_7[h,c]$

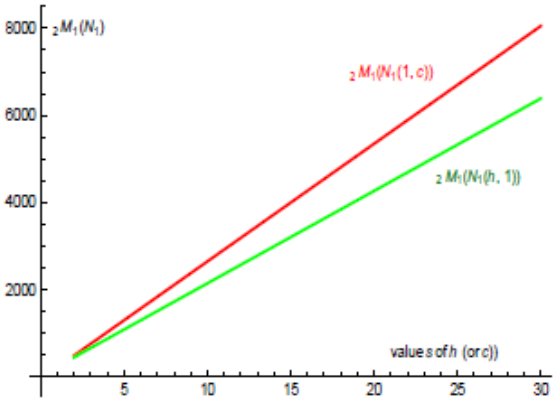

Figure 2: Graph of $_2M_1(N_1)$

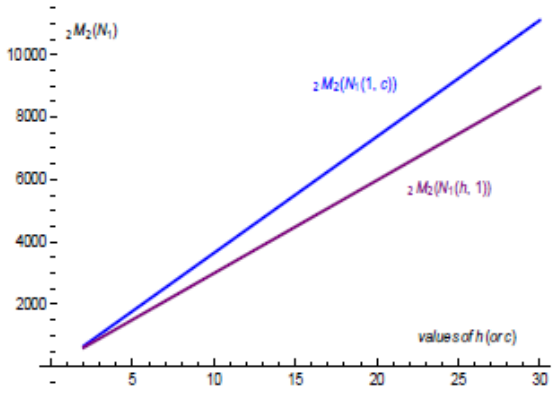

Figure 3: Graph of $_2M_2(N_1)$

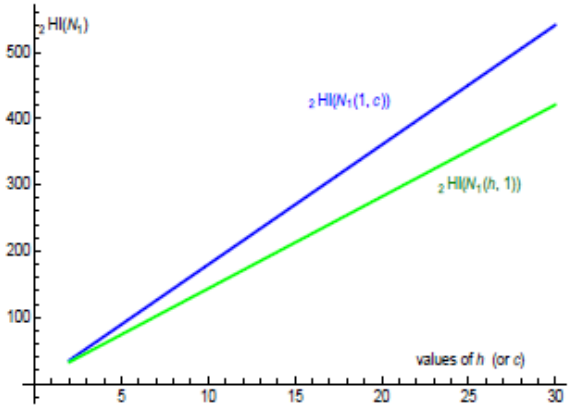

Figure 4: Graph of $_2HI(N_1)$

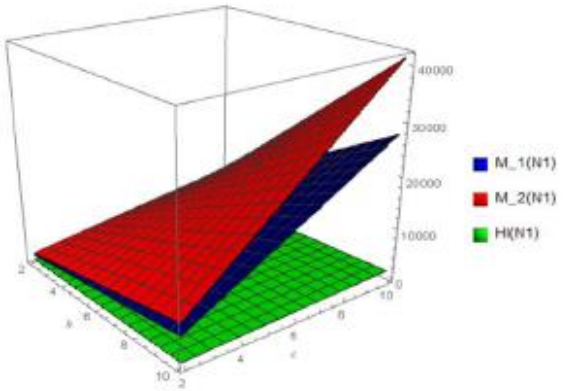

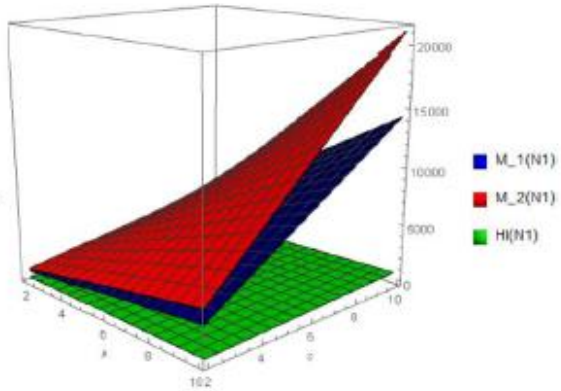

Figure 5: Graph of $_2M_1$,$_2M_2$ and $_2HI$ of $(N_1(h,c))$Figure 6: Graph of M_1, M_2 and HI of $(N_1(h,c))$

The analysis of the First Zagreb index, Second Zagreb index, and Harmonic index of VC_5C_7 are analysed based on the given values of $h(c = 1)$ or $c(h = 1)$. Figures 2, 3 and 4 depict these indices, where the x-axis represents the values of $h(c = 1)\ orc(h = 1)$, while $y - axis$ represents ${}_2M_1$, ${}_2M_2$ and ${}_2HI$ of VC_5C_7. Notably, ${}_2M_1$ ranges from 0 to 8000, ${}_2M_2$ from 0 to 10000 and ${}_2HI$ from 0 to 500, illustrating an increasing trend for all three indices as $h(c = 1)$ or $c(h = 1)$ increases. Furthermore, ${}_2M_1(N_1(1, c))$ exhibits a higher value compared to ${}_2M_1(N_1(h, 1))$. Among these indices, ${}_2M_2$ yields the highest value, surpassing the other First Zagreb and Harmonic indices.

The 3-dimensional graphs depicted in Figures 5 and 6 offer a visual representation wherein the index values for $l = 2$ precisely double when compared to the indices' values for $l = 1$. Despite this doubling effect, the fundamental nature of the graphs remains consistent for both $l = 1$ and $l = 2$. Notably, across both $l = 1$ and $l = 2$, the harmonic index consistently exhibits notably smaller values in comparison to the First and Second Zagreb indices.

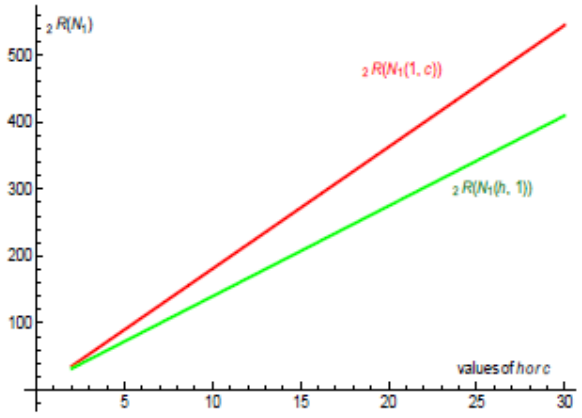

Figure 7: Graph of ${}_2R(N_1)$

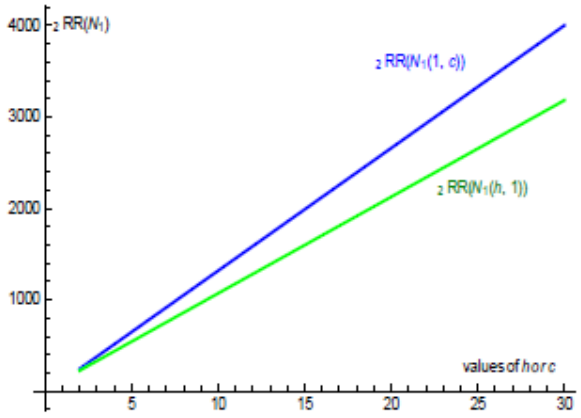

Figure 8: Graph of ${}_2RR(N_1)$

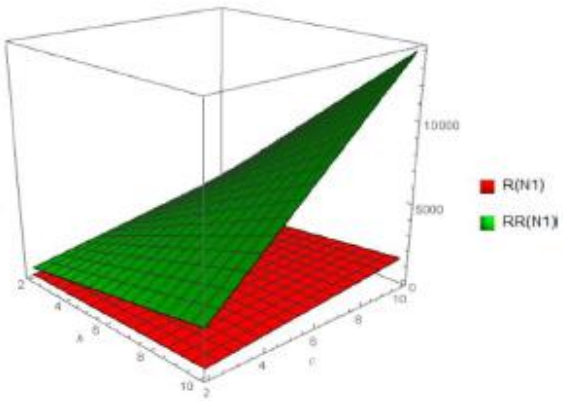

Figure 9: Graph of ${}_2R$ and ${}_2RR$ of $(N_1(h, c))$

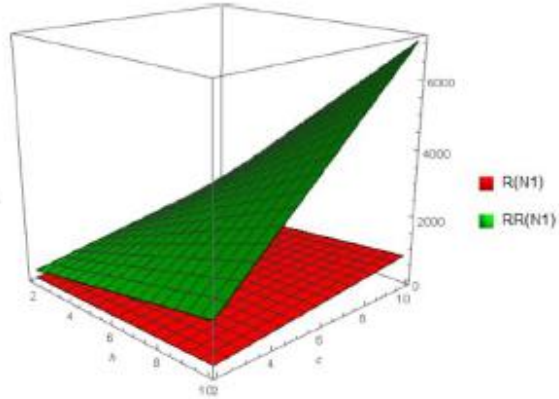

Figure 10: Graph of R and RR of $(N_1(h, c))$

Figures 7 and 8 illustrate the graphs of ${}_2R$ and ${}_2RR$ of VC_5C_7 respectively, with the values of $h(c = 1)$ or $c(h = 1)$ plotted along the x-axis. It is evident from the graphs that both indices exhibit an increasing trend, although ${}_2R$ increases at a slower rate compared to ${}_2RR$, which demonstrates a rapid increase in its values as h or c increases. Additionally, at all points where $h = c$, the value of ${}_2RR$ surpasses that of ${}_2R$ for VC_5C_7.

For a more comprehensive understanding, a 3-dimensional graph representing the Randić and Reciprocal Randić index of $VC_5C_7(h, c)$ is depicted in Figures 9 and 10. Here, the values of h (≥ 2) are plotted along the x-axis, while the values of c (≥ 2) are plotted along the y-axis for both $l = 1$

and $l = 2$. It is noteworthy that in both cases of l, the Reciprocal Randić index consistently exhibits the highest values, accompanied by a rapid increase, while the Randić index consistently yields the lowest values.

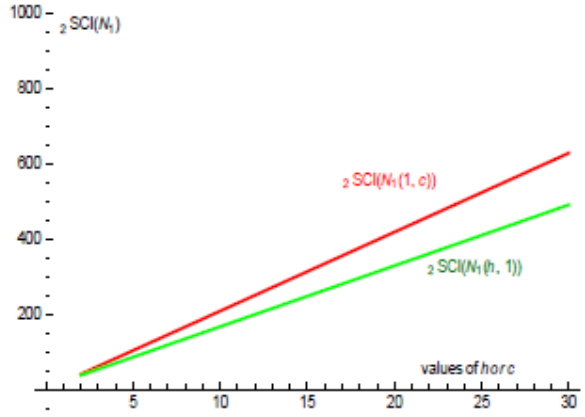

Figure 11: Graph of $_2SCI(N_1)$

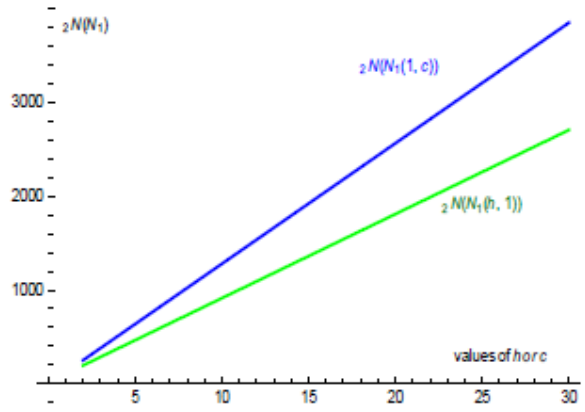

Figure 12: Graph of $_2N(N_1)$

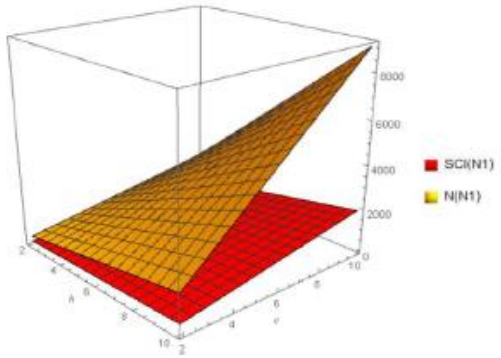

Figure 13: Graph of $_2SCI$ and $_2N$ of $(N_1(h,c))$

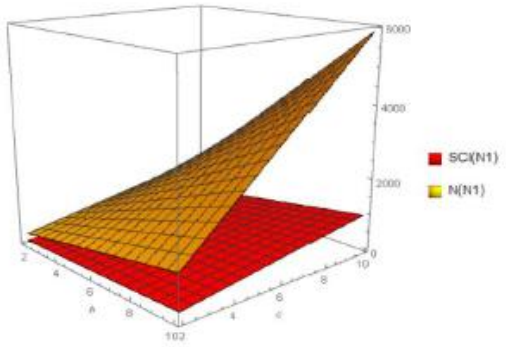

Figure 14: Graph of SCI and N of $(N_1(h,c))$

The analysis of the Sum Connectivity Index (SCI) and Nirmala Index of the molecular graph VC_5C_7 is conducted based on the provided values of $h(c = 1)$ or $c(h = 1)$. In Figures 11 and 12, these indices are illustrated, with the x-axis denoting the values of $h(c = 1)$ or $c(h = 1)$, and the y-axis representing $_2SCI(N_1)$ and $_2N$ of VC_5C_7. The $_2SCI(N_1)$ values range from 0 to 1000, while $_2N$ ranges from 0 to 4000, showcasing an increasing trend for both indices as $h(c = 1)$ or $c(h = 1)$ increases. Remarkably, $_2N(N_1(1,c))$ exhibits a higher value compared to $_2N(N_1(h,1))$ and $_2SCI(N_1(1,c))$ exhibits a higher value compared to $_2SCI(N_1(h,1))$, highlighting the varying magnitudes of these indices. Notably, among these indices, $_2N$ achieves the highest values, surpassing the Sum Connectivity indices.

In contrast, the 3-dimensional graphs depicted in Figures 13 and 14 illustrate a visual representation wherein the index values for $l = 2$ do not exhibit a significantly higher value when compared to the indices' values for $l = 1$. The fundamental characteristics of the graphs remain consistent for both $l = 1$ and $l = 2$. It's worth noting that, across both $l = 1$ and $l = 2$, the Nirmala Indices consistently exhibit higher values compared to the Sum Connectivity indices.

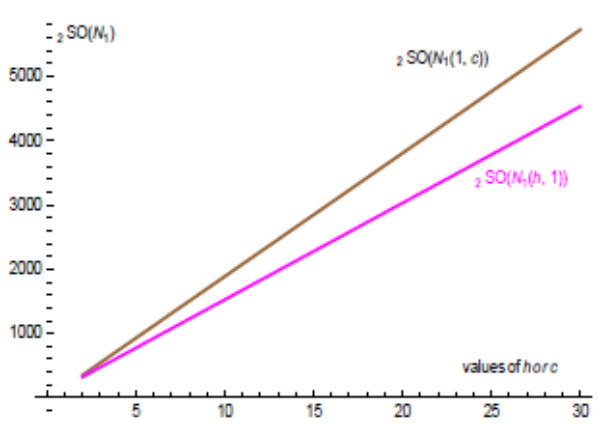

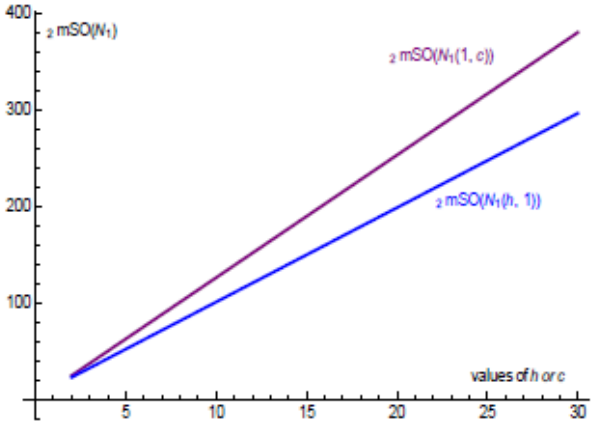

Figure 15: Graph of $_2SO(N_1)$Figure 16: Graph of $^m_2SO(N_1)$

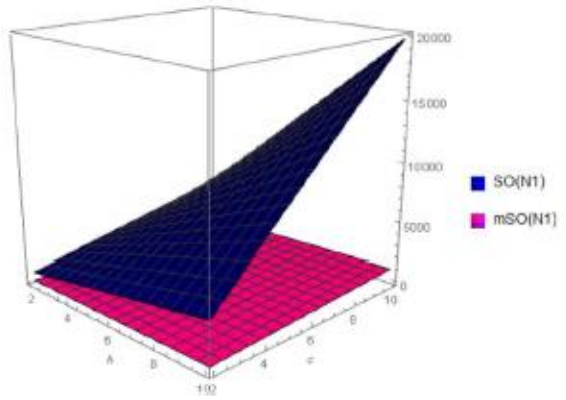

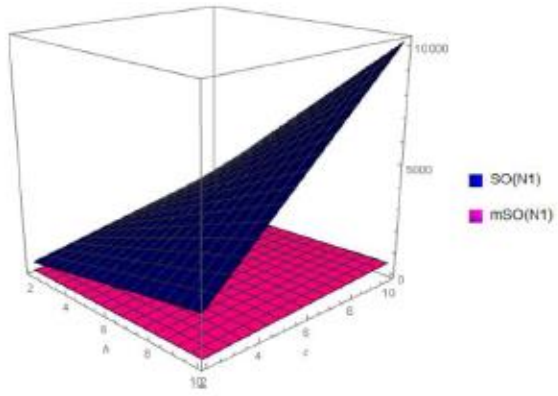

Figure 17: Graph of $_2SO$ and ^m_2SO of $(N_1(h,c))$ Figure 18: Graph of SO and ^mSO of $(N_1(h,c))$

The Sombor Index and Modified Sombor Index of the molecular graph VC_5C_7 are analyzed based on the provided values of $h(c=1)$ or $c(h=1)$. Figures 15 and 16 showcase these indices, where the x-axis corresponds to the values of $h(c=1)$ or $c(h=1)$, and the y-axis represents $_2SO(N_1)$ and $^m_2SO(N_1)$ of VC_5C_7. Across both indices, a distinct increasing trend is observed as $h(c=1)$ or $c(h=1)$ increases. Specifically, $_2SO(N_1)$ values range from 0 to 6000, while $^m_2SO(N_1)$ ranges from 0 to 400. Notably, when comparing values derived from different compositions of h and c, $_2SO$ tends to exhibit higher magnitudes compared to ^m_2SO. Moreover, the relative comparison between the indices' values remains consistent, with $_2SO$ consistently yielding higher values compared to ^m_2SO.

3-Dimensional visualizations presented in Figures 17 and 18 highlight how doubling the value of l from 1 to 2 results in a clear doubling effect on the indices' values. The fundamental features of the graphs remain consistent for both $l=1$ and $l=2$, with the Sombor Index consistently exhibiting significantly higher values compared to the Modified Sombor Index in both the conditions.

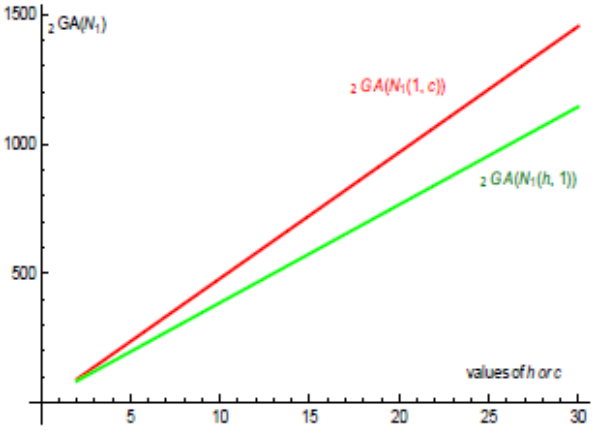

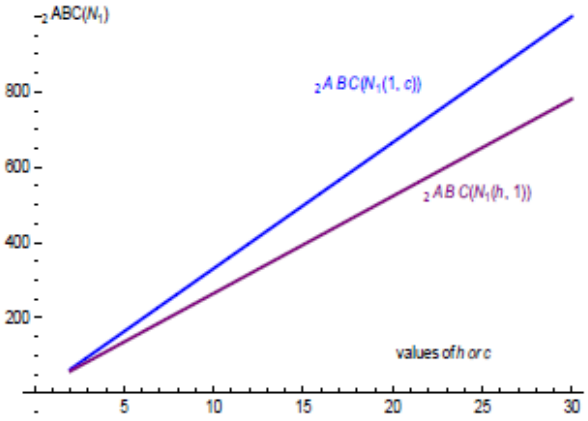

Figure 19: Graph of $_2GA(N_1)$ Figure 20: Graph of $_2ABC(N_1)$

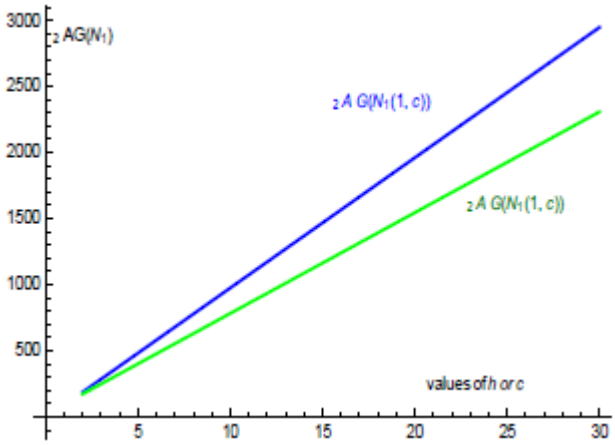

Figure 21: Graph of $_2AG(N_1)$

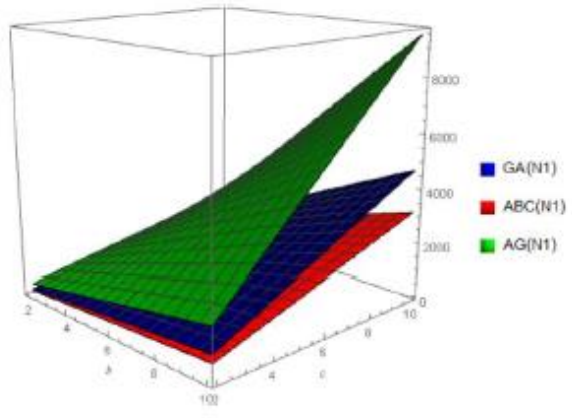

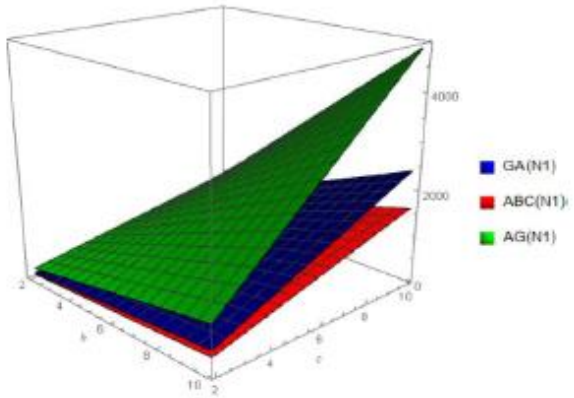

Figure 22: Graph of $_2GA$, $_2ABC$ and $_2AG$ of $(N_1(h,c)$Figure 23: Graph of GA, ABC and AG of$(N_1(h,c))$

In Figures 19, 20, and 21, the x-axis represents the values of $h(c = 1)$ or $c(h = 1)$, while the y-axis displays the values of $_2GA$, $_2ABC$, and $_2AG$ of VC_5C_7. Key observations from these graphs are as follows:

All three indices demonstrate a linearly increasing trend as $h(c = 1)$ or $c(h = 1)$ increases. ${}_2AG$ exhibits a notably rapid increase compared to ${}_2GA$ and ${}_2ABC$. Moving on to Figures 22 and 23, which illustrate 3D graphs of the Geometric-Arithmetic Index, Arithmetic-geometric Index, and Atom Bond Connectivity Index of $VC_5C_7(h,c)$ for $h,c \geq 2$, considering $l = 2$ and $l = 1$ respectively, the observations are as follows:

• In both cases of l, the Arithmetic-geometric Index displays the highest value and experiences the most rapid increase.

• the Atom Bond Connectivity Index consistently maintains the lowest value and demonstrates the slowest increase.

Moreover, the graphs reveal the following inequality: $ABC < {}_2ABC \leq GA < {}_2GA < AG \leq {}_2AG$. This inequality explains the varying magnitudes and trends across the different indices, offering valuable insights into their comparative behaviors.

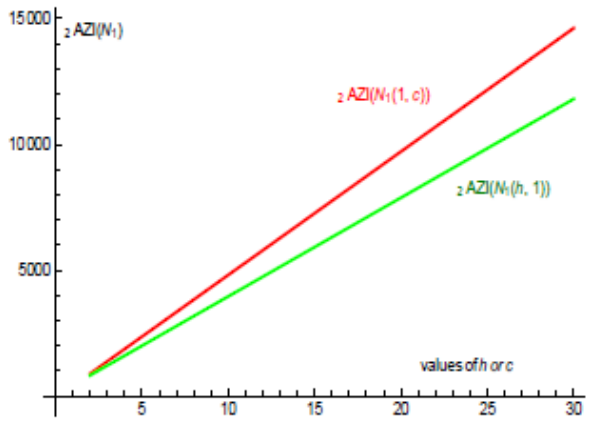

Figure 24: Graph of ${}_2AZI(N_1)$

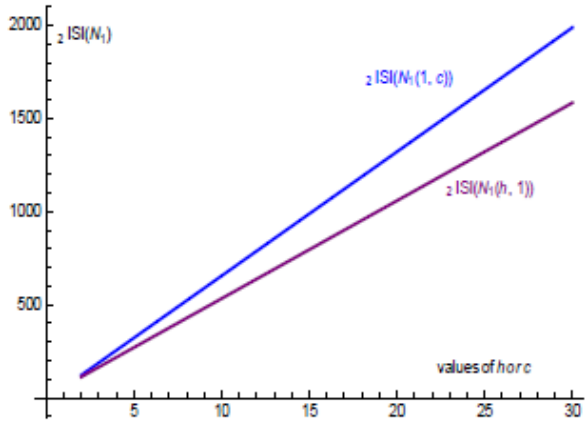

Figure 25: Graph of ${}_2ISI(N_1)$

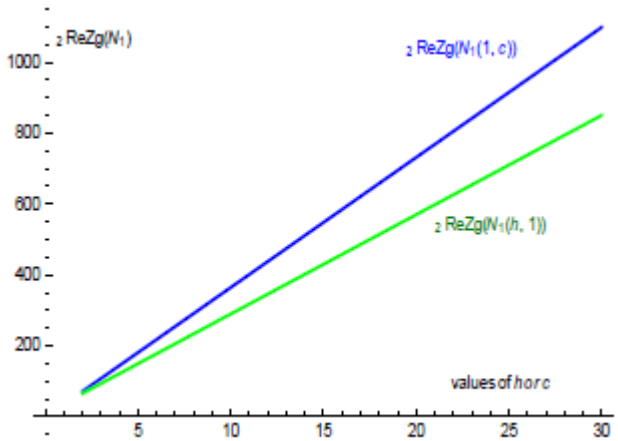

Figure 26: Graph of ${}_2ReZg(N_1)$

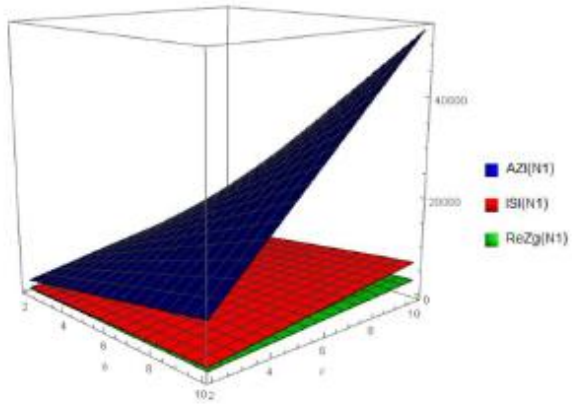

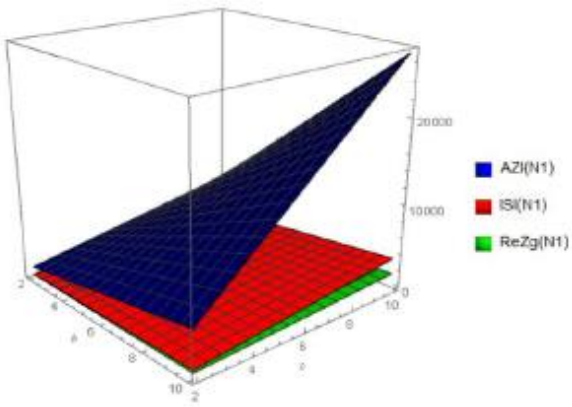

Figure 27: Graph of ${}_2AZI, {}_2ISI$ and ${}_2ReZg$of$(N_1(h,c))$Figure 28: Graph of $AZI, ISI$and $ReZg$of $(N_1(h,c))$

First Zagreb Index (ReZg) of VC_5C_7 are analyzed based on the provided values of $h(c=1)$ or $c(h=1)$. Figures 24, 25, and 26 shows these indices, where the x-axis represents the values of $h(c=1)$ or $c(h=1)$, and the y-axis represents ${}_2AZI$, ${}_2ISI$, and ${}_2ReZg$ of VC_5C_7.
Key observations from the analysis are as follows:

- ${}_2AZI$ ranges from 0 to 15000, ${}_2ISI$ from 0 to 2000, and ${}_2ReZg$ from 0 to 1000, illustrates that ${}_2AZI$ yields the highest values, exceeding a consistent increasing trend for all three indices as $h(c=1)$ or $c(h=1)$ increases.

- ${}_2AZI$, ${}_2ISI$, and ${}_2ReZg$ of $N_1(1,c)$ exhibit higher values compared to $N_1(h,1)$, indicating variations in index magnitudes based on different compositions of h and c.

The 3-dimensional graphs presented in Figures 27 and 28 demonstrate that when l is increased from 1 to 2, the index values precisely double. Despite this doubling effect, the fundamental characteristics of the graphs remain consistent for both $l=1$ and $l=2$. Notably, across both cases, the Redefined First Zagreb Index consistently exhibits in particular smaller values compared to the Augmented Zagreb Index and Inverse Sum Indeg Index.

5. Conclusion

In the analysis of carbon nanosheets, topological descriptors play a crucial role in characterizing their structural properties. These descriptors quantify various aspects of the molecular connectivity within the nanosheet, offering insights into its complexity and arrangement. When discussing topological descriptors, it's common to consider parameters such as the number of pentagons (h) and the number of repetitions (c) in the nanosheet structure.
In studies related to Quantitative Structure Activity Relationship (QSAR) modeling, these topological indices are frequently utilized to predict the biological activities of chemical compounds. By understanding how the structural features of carbon nanosheets influence these descriptors, researchers can gain valuable information about the nanosheet's potential biological effects or applications.
Upon examining graphs or data visualizations representing the behavior of these topological indices with changes in h and c, a consistent trend emerges: as both h and c increase, the values of these descriptors tend to rise. This suggests that larger h and c values correspond to more intricate and potentially complex molecular structures within the nanosheet.
However, a more nuanced observation arises when comparing the impact of varying c while keeping h constant versus altering h while c remains consistent. It becomes evident that changes in

the number of repetitions (c) have a more significant effect on these topological indices compared to alterations in the number of pentagons (h). This implies that increasing the number of repetitions in the carbon nanosheet structure has a disproportionate impact on the overall connectivity, symmetry, or structural arrangement of the nanosheet, leading to more pronounced changes in the topological descriptors.

This insight suggests that the repetition pattern within the nanosheet structure plays a crucial role in determining its topological properties. The observed pattern underscores the importance of considering not only the individual structural features but also their collective arrangement and repetition in understanding the behavior of carbon nanosheets in various applications and contexts.

This suggests that the structural attributes captured by the topological indices exhibit comparability or consistency when comparing distances 1 and 2 in the examined graph. Such an observation offers valuable insights into the interrelations and patterns within the network across various spatial scales or levels of connectivity.

References

[1] I. Gutman, N. Trinajsti´c, *Graph theory and molecular orbitals. III. Total p-electron energy of alternate hydrocarbons*, Chem. Phys. Lett, **17** (1972), 535–538.

[2] Akbar Ali, Suresh Elumalai, Shaohui Wang, Darko Dimitrov, *On the Bicyclic Graphs with Minimum Reduced Reciprocal Randić Index*, Iranian J. Math. Chem. **9** (3) (2018), 227 – 239.

[3] Hafiza Bushra Mumtaz, Muhammad Javaid,Hafiz Muhammad Awais, Ebenezer Bonyah, *Topological Indices of Pent-Heptagonal Nanosheets via M-Polynomials*, J. Math. Vol. (2021), Article ID 4863993, 13 pages. https://doi.org/10.1155/2021/4863993.

[4] Fei Deng, Xiujun Zhang, Mehdi Alaeiyan, Abid Mehboob, and Mohammad Reza Farahani, *Topological Indices of the Pent-Heptagonal Nanosheets VC5C7 and HC5C7*, Adv.Mater. Sci. Eng. Vol 2019, Article ID 9594549, 12 pages.

[5] E. Estrada, L. Torres, L. Rodrguez, and I. Gutman, *An atom-bond connectivity index: modeling the enthalpy of formation of alkanes*,Indian J. Chem. A, **vol. 37**(1998), 849–855.

[6] S. Ediz, *On ve-degree molecular topological properties of silicate and oxgen networks*,Int. J. Comput. Sci. Math., 9(1) (2018), 1-12.

[7] M. R. Farahani, *Connectivity indices of pent-heptagonal nanotubes VAC5C7[p,q]*, Adv. Mater. Corros., **2(1)** (2013), 33–35.

[8] B. Furtula, A. Graovac, and D. Vukičević, *Augmented Zagreb index*, J. Math. Chem., **48(2)** (2010),370–380.

[9] I. Gutman, B. Furtula, C. Elphick, *Three new/old vertex-degree-based topological indices*, MATCH Commun. Math. Comput. Chem. **72** (2014) 617–632.

[10] Yingying Gao, Wasim sajjad, Abdul Qudair Baig, Mohammed Reza Farahani,*The Edge Version of Randic, Zagreb, Atom Bond Connectivity and Geometric-Arithmetic indices of HAC5C6C7 nanotube*,Int. J. Pure Appl. Math. **115(2)** (2017) 405-418.

[11] F. C. G. Manso, H. S. Júnior, R. E. Bruns, A. F. Rubira, E. C. Muniz, *Development of a new topological index for the prediction of normal boiling point temperatures of hydrocarbons: The Fi index*, J. Mol. Liquids, **165** (2012) 125–132. 22.

[12] I.Z. Raza and E. K. Sukaiti, *M-polynomial and degree based topological indices of some nanostructures*, Symmetry, **12(5)** (2020), 831.

[13] G. R. Roshini and S. B. Chandrakala, *Multiplicative Zagreb Indices of Transformation Graphs, Anusandhana*, J. Sci. Eng. Manage. **6 (1)** (2018), 18-30.

[14] G. R. Roshini, S. B. Chandrakala and B. Sooryanarayana, *some degree based topological indices of transformation graphs, Bull*, Int. Math. Virtual Inst. **10 (2)** (2020), 225-237.

[15] B. Sooryanarayana, S. B. Chandrakala and G. R. Roshini, *On Realization and Characterization of Topological Indices*, Int. J. Innovat. Technol. Explor. Eng. **9 (1)** (2019), 715-718.

[16] Sooryanarayana, B., S. B. Chandrakala, and G. R. Roshini, *Zagreb indices at a distance 2*, J. Math. Comput. Sci. C, **10.3**(2020), 639-655. https://doi.org/10.28919/jmcs/4396.
[17] X. Zhang, W. Sajjad, A. Q. Baig, and M. R. Farahani, *The edge version of degree based topological indices of p NAqp nanotube*, Appl. Math., **08(10)** (2017) 1445–1453.
[18] B. Zhou and N. Trinajstic, *On a novel connectivity index*, J. Math. Chem., **46(4)** (2009), 1252–1270.
[19] Yang,Z., Shi, L., Wang, H., Xiong, J., Xu, X., Sun, L., Jiang, J., Zhuang, Q., Chen, Y., and Ju, Z., *Crystallization-induced thickness tuning of carbon nanosheets for fast potassium storage*, J. Colloid Interface Sci, **53(6)** (2023), 30-38.
[20] B. Zhou and N. Trinajstic, *On general sum-connectivity index*, J.Math. Chem., **47(1)** (2010), 210–218.